SPR DETECTION OF SINGLE NANO PARTICLES AND VIRUSES

Alexander Zybin
ISAS - Institut for Analytical Science, Bunsen-Kirchhoff-Strasse 11, 44139 Dortmund, Germany
zybin@isas.de

Evgeny L. Gurevich
ISAS - Institut for Analytical Science, Bunsen-Kirchhoff-Strasse 11, 44139 Dortmund, Germany

Frank Weichert
Department of Computer Science VII, Dortmund University of Technology, Germany

Kay Niemax
ISAS - Institut for Analytical Science, Bunsen-Kirchhoff-Strasse 11, 44139 Dortmund, Germany

Abstract
Here we report a novel method for detection of single individual particles and viruses by means of surface plasmon assisted optical microscopy. The size of the studied objects may be at least one order of magnitude less than the wavelength of the light used for the imaging. This allows studying of nanoparticles and viruses in natural surrounding (enviroment) by means of cheap and well-developed visible-light sources. The signal reflected from the nanoparticle is enhanced due to excitation of the surface plasmon polariton waves. Combination with modern image-processing procedure allows automatic detection of nano-sized objects.

Key words
Surface Plasmon Resonance, nano particles, viruses, detection

1 Introduction

By applying the conventional optical microscopy to detection of particles, which are smaller than the wavelength, scattered light is observed. Since the scattering cross section drops as six power of the size, high illumination intensity and high aperture objective is required. In the present work a new approach for nano particles visualization is suggested. The observation of the particle is based on local growing of reflection on a surface caused by a particle bound to the surface. The reflection is observed on a thin metal layer in the Kretschman scheme for surface plasmon resonance measurements. It was shown that the local reflection signal increasing corresponds to effective scattering cross section which is by up to three orders of magnitude larger than by Mie scattering on the same particle. It turns out that the light intensity change on the image, caused by binding of a particle, is much bigger than intuitively expected by taking into account only the higher reflectivity on the affected area. This amplification is caused by the interference of the particle initiated light with the light reflected at the gold surface in the vicinity of the particle. Since these two field are coherent the amplitudes should be summarized instead of simple summarizing of intensities as intuitively expected. Resulting particles with the diameter below 40 nm can be observed. The method was tested and optimized by detection of polistyrol nanoparticles and finally applied for virus detection.

The suggested method needs that particles are bound on the sensor surface. This provides the opportunity to detect selectively the particles of interest. Foe example coating the sensor surface with antibodies to a definite virus provides detection of only one selected type of viruses. The advantage of the method is that any individual virus is detected as soon as it is caught by the surface receptor layer. This provides very high concentration sensitivity. First experimental data show that viruses in a sample with the concentration of 1000

V/ml can be detected in one hour.

The suggested approach applies the Kretschmann scheme in imaging mode with CCD detection. The sensor surface was illuminated with a parallel beam and the area of interest was imaged onto the CCD chip. The incidence angle was chosen on the slop of the reflectance curve, so that the reflectivity grew by binding of a particle.

2 Experimental set-up

The experimental set-up is shown in the Figure 1. The Kretschmann configuration in imaging mode (Röthenhäuser and Knoll, 1988) was applied. A glass slide covered by a 50 nm thick gold layer was attached with immersion oil to a prism. The gold layer was illuminated trough the prism at a fixed incidence angle by superluminescent diode (QSDM-680-9 from QPhotonix, wavelength 670 nm) in order to avoid a specle structure appearing by laser illumination. The incidence angle was chosen in such a way that the diode wavelengths was on the left (smaller angle) slope of the resonance minimum. The flow-cell attached to the gold layer was formed by a 1 mm thick, S-shaped PDMS sealing. The flow-cell back was made of a Plexiglas. It had two pipes served as in- and outlet. The flow-cell volume was about 300 μL.

Standard Minolta photo objective with the aperture 1/1.7 was used for imaging of the sensor surface onto the Solution 10001000 pixels CCD camera Kappa 100 with pixel size 6.45 $\times$ 6.45 μm. The magnification of $\times$7 was chosen so that one pixel corresponded to 1m on the sensor surface. However, in horizontal plane (p-plane) the image was compressed due to the slop of the sensor surface to the optical axes and one pixel corresponded to $\sim$1.4. The images were saved with the frame rate of up to 50 fr/s and automatically processed as described below.

At first the background is removed in order to separate relevant intensity patterns from irrelevant variations caused by experimental setting properties. Simplistically assuming a stationary background allows a constant reference image constructed by averaging the first B images (e.g. B=20) to be used via dividing each image by the reference image. To eliminate broad intensity fluctuations stemming from an actually nonstationary background, the intensity mean and variance of each image needs to be standardized.

Secondly, application specific discriminative features of the one dimensional temporal intensity profile at each pixel are used to classify the image in a region growing manner. Therefore a remaining broad-scale intensity trend is removed via subtracting a fitted low order polynomial, after which the maximum difference quotient of the profile is tresholded to classify the profile. To incorporate the typical spatial extent of relevant temporal intensity variations, each image is either median or morphologically filtered before profile analysis, which removes particle-like intensity profiles of little

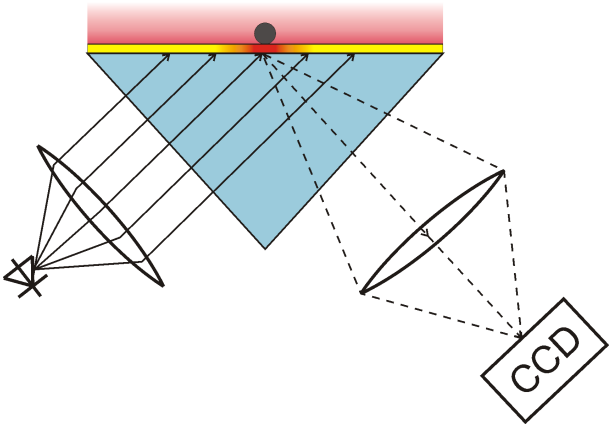

Figure 1. Experimental setup

spatial extend. Resulting neighboring particle positions are aggregated by outlining polygons using marching squares, and the polygons are lastly filtered using application specific features of shape to yield a final set of outlined virus positions.

3 Results and discussion

3.1 Measuring procedure

Two types of binding were used in order to fix particles on the surface: for biotin functionalized particles the surface was coated with streptavidin monolayer, for sulfate coated particles (negative charge) the surface was coated with $Al(OH)_3Cl$.

The incidence angle was tuned to the left slope of the reflection curve near to the resonance minimum. Buffer solution containing 0.1% NaCl was pumped in a cycle during 2-3 min to obtain a stable image. The pump velocity was of 0.3 ml/min. The diluted suspension of particles was than injected in the cycle. By binding a particle on the sensor surface a corresponding pattern appears on the image Figure 2a. The picture averaged over several frames, obtained before the particle suspension was coming, was used as the background image. This picture was subtracted from the following frames in order to get rid of the cross-section non-homogeneity of the reflected beam and to improve the contrast. In order to quantify the signal the *black* and *white* areas were selected at the images with a bound particle. In both areas the value:

$$S = \frac{\Sigma_{n=1}^{N} P_n}{N}$$

was taken as a signal for the corresponding area at the processed frame. P_n is the signal in the n-th pixel, and N is the number of pixels in the selected area.

The signals were calculated in every frame and the time dependences were plotted. Finally, the difference of the *black* and *white* signals was calculated and plotted. An example of the signals for different particles diameters are shown in the Figure 2(b). Figure 2(c)

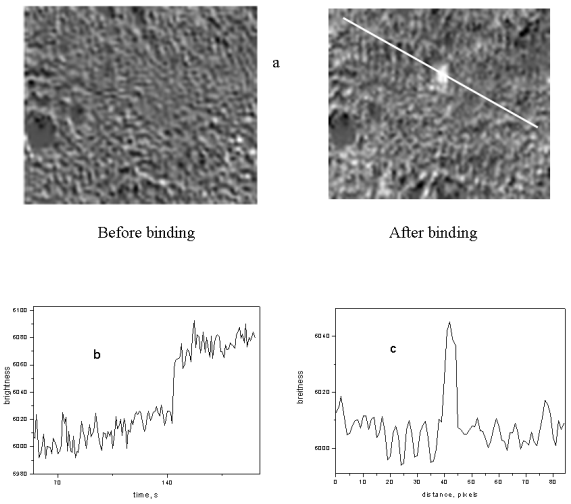

Figure 2. Binding of nanoparticles to the surface

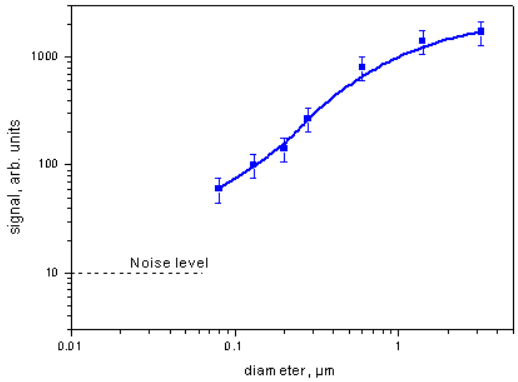

Figure 3. Dependence of the reflected signal on the particle diameter

shows the brightness profile along the white line on the figure 2(a).

3.2 Signal dependence on the particle diameter

The dependence of the signal on the particle diameter is shown in Figure 3. The smallest detected particles with diameter of 40 nm were detected with the S/N ratio of about 4.

A particle in a sample solution can be detected only after binding on the sensor surface. The particle can achieve the surface due to the Brownian motion. The Brownian displacement of a particle along the x axis during the time interval t is given by:

$$x = \sqrt{\frac{kTt}{3\pi\chi d}}$$

were k-Boltzmann constant, T- temperature, χ - water viscosity, d- particle diameter.

A particle with the diameter of 100 nm needs about 100 sec. to move 20 μm along a definite axis. Therefore, a particle travels from one side of a water layer of flow cell with the thickness of 20 μm to the other one and touches the sensor surface with 50% probability. Taking the sensor area 2×2 mm^2 one needs about 120 sec. in order to pump a 0.1 μl sample through the cell with the velocity which provides the 50% probability of the virus capture.

An important characteristic of the method is the smallest detectable particle. In the present work the smallest observed particles had the diameter of 40 nm. The S/N ratio was of about 5 by averaging over $\sim$10 s by the frame rate of $\sim$50 fps. The signals corresponding to the black and white spots were averaged over the areas corresponding to about 10 pixels. The middle pixel charge was about 6000 photoelectrons. This corresponds to the expected shot noise of $\sim$4 photoelectrons or relative signal fluctuations of 6×10^{-4}. This corresponds approximately to the noise in our measurements.

3.3 Feature based nanoparticle detection

To significantly enhance the separation of relevant intensity patterns from disturbing background variations in the future, the oversimplifying assumption of a stationary background needs to be removed by directly modeling a nonstationary background either stochastically or by using an adaptively varying background image.

In the future, the set of discriminative features of a temporal intensity profile has to be extended to incorporate more robust features by using a general signal analysis approach. Additionally, instead of merely analyzing temporal variations, the spatio-temporal variation of intensity needs to be modeled via either multivariate time series analysis or multidimensional time-frequency decompositions.

In order to estimate model parameters that are optimal in particle detection sense, the machine learning approach will be used the automatically set-up and tune the detection system.

4 Conclusion

The studies reported here demonstrate that the signal of binding of single nanoparticles to the SPR-sensor surface is significantly larger than intuitively expected. This makes it possible to observe binding of nanoparticles smaller than 40 nm. Since many viruses have the size of 30-200 nm the method can be applied to the virus diagnostics.

References

Röthenhäuser, B. and W. Knoll (1988). Surface plasmon microscopy. *Nature* **332**, 615.